ELSEVIER

Biochimica et Biophysica Acta 1418 (1999) 48–60

BIOCHIMICA ET BIOPHYSICA ACTA
BBA

Regulation of Ca^{2+} transport by sarcoplasmic reticulum Ca^{2+}-ATPase at limiting [Ca^{2+}]

Mervyn C. Berman *

Department of Chemical Pathology, University of Cape Town Medical School, Observatory 7925, Cape Town, South Africa

Received 2 October 1998; received in revised form 4 January 1999; accepted 28 January 1999

Abstract

The factors regulating Ca^{2+} transport by isolated sarcoplasmic reticulum (SR) vesicles have been studied using the fluorescent indicator Fluo-3 to monitor extravesicular free [Ca^{2+}]. ATP, in the presence of 5 mM oxalate, which clamps intravesicular [Ca^{2+}] at approximately 10 μM, induced a rapid decline in Fluo-3 fluorescence to reach a limiting steady state level. This corresponds to a residual medium [Ca^{2+}] of 100 to 200 nM, and has been defined as $[Ca^{2+}]_{lim}$, whilst thermodynamic considerations predict a level of less than 1 nM. This value is similar to that measured in intact muscle with Ca^{2+} fluophores, where it is presumed that sarcoplasmic free [Ca^{2+}] is a balance between pump and leaks. Fluorescence of Fluo-3 at $[Ca^{2+}]_{lim}$ was decreased 70% to 80% by histidine, imidazole and cysteine. The $K_{0.5}$ value for histidine was 3 mM, suggesting that residual $[Ca^{2+}]_{lim}$ fluorescence is due to Zn^{2+}. The level of Zn^{2+} in preparations of SR vesicles, measured by atomic absorption, was 0.47 ± 0.04 nmol/mg, corresponding to 0.1 mol per mol Ca-ATPase. This is in agreement with findings of Papp et al. (Arch. Biochem. Biophys., 243 (1985) 254–263). Histidine, 20 mM, included in the buffer, gave a corrected value for $[Ca^{2+}]_{lim}$ of 49 ± 1.8 nM, which is still higher than predicted on thermodynamic grounds. A possible 'pump/leak' mechanism was tested by the effects of varying active Ca^{2+} transport 1 to 2 orders with temperature and pH. $[Ca^{2+}]_{lim}$ remained relatively constant under these conditions. Alternate substrates acetyl phosphate and *p*-NPP gave similar $[Ca^{2+}]_{lim}$ levels even though the latter substrate supported transport 500-fold slower than with ATP. In fact, $[Ca^{2+}]_{lim}$ was lower with 10 mM *p*-NPP than with 5 mM ATP. The magnitude of passive efflux from Ca-oxalate loaded SR during the steady state of $[Ca^{2+}]_{lim}$ was estimated by the unidirectional flux of $^{45}Ca^{2+}$, and directly, following depletion of ATP, by measuring release of $^{40}Ca^{2+}$, and was 0.02% of V_{max}. Constant infusion of $CaCl_2$ at $[Ca^{2+}]_{lim}$ resulted in a new steady state, in which active transport into SR vesicles balances the infusion rate. Varying infusion rates allows determination of [Ca^{2+}]-dependence of transport in the absence of chelating agents. Parameters of non-linear regression were $V_{max} = 853$ nmol/min per mg, $K_{0.5(Ca)} = 279$ nM, and $n_{H(Ca)} = 1.89$. Since conditions employed in this study are similar to those in the sarcoplasm of relaxed muscle, it is suggested that histidine, added to media in studies of intracellular Ca^{2+} transients, and in the relaxed state, will minimise contribution of Zn^{2+} to fluophore fluorescence, since it occurs at levels predicted in this study to cause significant overestimation of cytoplasmic free [Ca^{2+}] in the relaxed state. Similar precautions may apply to non-muscle cells

Abbreviations: AcP, acetyl phosphate; $[Ca^{2+}]_{lim}$, limiting concentration of medium or cytosolic free calcium ions; DMSO, dimethyl sulfoxide; E-P, phosphorylated forms of the Ca^{2+}-ATPase; EGTA, ethyleneglycol bis(β-amino ethyl ether)-*N,N,N′,N′*-tetraacetic acid; F_{lim}, Fluorescence of fluophore, Fluo-3, at limiting [Ca^{2+}]; F_{min} and F_{max}, Fluorescence of Fluo-3 with excess EGTA and with saturating [Ca^{2+}]; MOPS, 3-(*N*-morpholino)propanesulfonic acid; *p*-NPP, *p*-nitrophenyl phosphate; SDS–PAGE, sodium dodecyl sulphate–polyacrylamide gel electrophoresis; SR, sarcoplasmic reticulum

* Fax: +27-21-448-8150; E-mail: mervyn@chempath.uct.ac.za

0005-2736/99/$ – see front matter
PII: S0005-2736(99)00017-6

as well. This study also suggests that $[Ca^{2+}]_{lim}$ in the resting state is a characteristic feature of Ca^{2+} pump function, rather than a balance between active transport and passive leakage pathways.

Keywords: Ca^{2+} transport; Sarcoplastic reticulum

1. Introduction

Sarcoplasmic and endoplasmic reticulum Ca^{2+}-ATPases (SERCAs) are present in all nucleated mammalian cells and function as calcium pumps to restore cytoplasmic Ca^{2+} levels following stimuli that are mediated by calcium signalling, and are therefore responsible for regulating resting levels of cytoplasmic $[Ca^{2+}]$. The Ca^{2+}-ATPase of skeletal muscle has been particularly well studied and characterised, and is perhaps one of the best understood examples of energy transduction, in which chemical energy of ATP is converted into the energy of an osmotic gradient [1–6]. Isolated vesicles from rabbit skeletal muscle sarcoplasmic reticulum (SR) are particularly suitable for transport and energy coupling studies. They are obtained in high yield, with $>80\%$ purity of Ca^{2+}-ATPase pump protein, are physiologically orientated with cytoplasmic surface outwards, and are tightly sealed.

Early studies, using steady state flux ratios for ATP hydrolysis and calcium transport, showed Ca/ATP ratios that approached 2, suggesting that two Ca^{2+} ions are translocated per pump cycle [1]. This is in agreement with passive binding studies, which have characterised two high affinity Ca^{2+} binding sites facing the cytoplasmic surface of SR membranes [7]. Although there is not complete agreement with respect to all the intermediate states of the catalytic cycle [8], it appears that all of the partial reactions can be accomplished by the 110 kDa pump monomer [9], and that following binding of cytoplasmic Ca^{2+}, phosphorylation to form E-P leads to occlusion of the two transported cations. Subsequent reorientation and decrease in affinity of the transport sites leads to deocclusion and release of the two calcium ions onto the lumenal surface of SR membranes [10]. A single unbranched catalytic cycle, originally proposed by de Meis and Vianna [11], is consistent with this model and with tight coupling of transport to ATP hydrolysis. This view is consistent with the apparent equilibrium state of the SR Ca^{2+}-ATPase under physiological conditions in vivo and in vitro [12].

Previous reports on the $[Ca^{2+}]$-dependence of transport by isolated SR, showing Hill coefficients of two lead to the consensus that occupation of two Ca^{2+} sites is required both for the activation of catalysis and of transport, and that this 2:1 coupling ratio was maintained over a wide Ca^{2+} concentration range [13], where Ca^{2+} buffers, usually CaEGTA, were used to vary free $[Ca^{2+}]$ in the submicromolar range. However, EGTA and/or CaEGTA have been shown to enhance the apparent affinity of the Ca^{2+} pump [14]. The $[Ca^{2+}]$-dependence of transport has been estimated in the absence of chelators by Klein et al. [15], from the decline in myoplasmic Ca^{2+} following contraction in skinned frog skeletal muscle, and they have proposed that the high cooperativity ($n_H = 3.6$) favours a functional pump dimer.

Coupling ratios, in the absence of EGTA, decline in the submicromolar Ca^{2+} range from 2.0 to near zero, implying that the pump may 'slip' under these conditions [16]. Inesi and de Meis [17] have described slippage when transport into isolated SR vesicles is limited by high intravesicular $[Ca^{2+}]$ and 10 000:1 gradient, conditions referred to as 'static head'.

The Ca^{2+} pump of SR is in thermodynamic equilibrium in the physiological state [12]. The present study of Ca^{2+} transport by isolated SR vesicles has been characterised, using the fluophore, Fluo-3 [18], at low free external calcium ion concentrations that are limiting for Ca^{2+} ($[Ca^{2+}]_{lim}$), without the constraint of a significant concentration gradient. In the presence of oxalate both external high affinity and internal low affinity calcium binding sites are expected to be vacant. Interference from Zn^{2+} has been minimised with a histidine buffer. Ca^{2+} concentration dependence of transport, determined in the absence of EGTA, is cooperative, with a Hill coefficient approaching 2, suggesting that the monomeric Ca^{2+}-ATPase is competent to form an isolated pump unit.

2. Materials and methods

2.1. Materials

The sources of materials were as follows: ATP, Sigma; amylase, Boehringer Mannheim. Standardised 100 mM $CaCl_2$ solution was prepared from Analar $CaCO_3$, adjusted to pH 5.6 with 1 M HCl. The penta-ammonium salt of Fluo-3, lot number 2641-4, was obtained from Molecular Probes (Eugene, OR, USA). A 1-mM stock solution was made up in DMSO and kept at −20°C in the dark.

2.2. Preparation of skeletal muscle sarcoplasmic reticulum vesicles

Isolated sarcoplasmic reticulum vesicles were prepared from the back and hind leg muscle of white rabbits by the method of Champeil et al. [19]. Amylase, 1 μg/ml, was added to the initial homogenate in order to decrease glycogen content and phosphorylase contamination to less than 5%, as determined by PAGE [20]. Protein concentrations were determined from the optical absorbance at 280 nm in 50 mM sodium phosphate (pH 7.0), 1% (w/v) sodium dodecyl sulfate [19]. Suspensions of SR vesicles, 35 to 40 mg/ml, were stored at −70°C.

2.3. Determination of steady state levels of extravesicular [Ca^{2+}], Ca^{2+} uptake and release

The kinetics of calcium uptake and release, and of steady-state levels of extravesicular free [Ca^{2+}] were monitored under standard conditions at 25°C in medium containing 20 mM MOPS–Tris (pH 6.8), 5 mM $MgCl_2$, 5 mM sodium oxalate, and 20 nM Fluo-3. The final concentration of SR vesicles was maintained at 0.25 mg protein per ml for all experiments. Fluorescence was recorded in a 1 cm cuvette with continuous magnetic stirring, using a SPEX 'Fluoromax' spectrofluorimeter, with excitation at 509 nm and emission of 535 nm. Maximum fluorescence, F_{max}, was established by preincubation with 20 μM $CaCl_2$, prior to addition of 2 mM ATP, unless otherwise stated.

Free [Ca^{2+}] was calculated from the observed fluorescence, F, according to the equation

$$[Ca^{2+}]_{free} = K_d(F-F_{min})/(F_{max}-F)) \quad (1)$$

assuming K_ds for Ca^{2+} binding of 450 nM at 25°C [18], and of 864 nM at 37°C [21]. For purposes of calculation of $[Ca^{2+}]_{free}$, the K_d was assumed to remain constant between 10°C and 25°C, and increase linearly up to 42°C.

V_{max} of Ca^{2+} transport was measured by monitoring $[Ca^{2+}]_{free}$ following rapid injection of 100 μM $CaCl_2$ into the cuvette. The reciprocal of the time taken for $[Ca^{2+}]_{free}$ to return to the midpoint between F_{max} and F_{min} was used to calculate V_{max}, since during the major fraction of the timed period $[Ca^{2+}]_{free}$ would be near to saturation of high affinity Ca^{2+} binding by the Ca^{2+}-ATPase.

Ca^{2+}-dependence of transport was determined by a constant infusion method. SR vesicles were incubated with 20 μM Ca^{2+} and 2 mM ATP for 100 s, during which time a steady state at $[Ca^{2+}]_{lim}$ was established. Infusion of 5 mM or 50 mM standardised $CaCl_2$ was added, with continuous magnetic stirring, by means of a Welmed P1000 constant infusion pump fitted with a 1-ml syringe. The resulting pseudo-steady-state of $[Ca^{2+}]_{free}$ was extrapolated back to t_0, the time of beginning of infusion. Transport is assumed to be equal to infusion rate during steady state.

2.4. Determination of Zn^{2+} content of preparations of SR vesicles

Suspensions of SR vesicles, 25 to 35 mg/ml, were diluted 1:1 with 10% TCA, mixed and allowed to stand a room temperature for 10–15 min. The mixture was centrifuged at 3000 rpm and the supernatant analysed in a Varian AA10 Atomic Absorption spectrophotometer. Standards of 4 to 24 μM Zn^{2+} were prepared from a 1-mM Commercial zinc acetate solution.

3. Results

3.1. Factors determining limiting medium [Ca^{2+}] during Ca^{2+} uptake into isolated SR vesicles

Initial experiments were carried out to investigate the suitability of Fluo-3 as a probe of medium or

extravesicular free [Ca^{2+}]. In order to meet these criteria, Fluo-3 fluorescence should be derived from a single pool of Ca^{2+}–Fluo-3, with minimum contribution from intravesicular Ca^{2+}, or deviation from ideal behaviour due to binding to SR vesicular membranes or glassware. Suitable fluorescence signals could be recorded with minimum noise from 20 nM total dye concentration. Excitation and emission spectra from Fluo-3, saturated with excess Ca^{2+} (F_{max}), with excess EGTA (F_{min}), and from media depleted of Ca^{2+} by active transport into vesicles in the presence of oxalate (F_{lim}) are shown in Fig. 1. These spectra, taken at 10-fold higher concentrations of Fluo-3 to exclude non-ideal behaviour, illustrate the large increase in fluorescence with maximum excitation at 509 nm, and emission at 530 nm, between F_{min} and F_{max}. Spectra at F_{lim} show peaks at identical wavelengths, and no evidence of shifts due to bound dye species, or of more than a single pool of the fluophore. In all further experiments 20 nM Fluo-3 was used to eliminate any possibility of Ca^{2+}–Fluo-3 interaction with the Ca^{2+}-ATPase. The contribution of autofluorescence by vesicles of 0.83% of F_{max} was minimal, whilst fluorescence due to Ca^{2+} binding to Fluo-3 was 97.7% of F_{max}. It appears, therefore, that Fluo-3 behaves as an ideal free [Ca^{2+}] indicator, especially as its useful concentration of 20 nM is much lower than that of the CaATPase (0.25 mg/ml or $\cong$1 μM), and would have little Ca^{2+}-buffering effect.

SR vesicles are able to sequester appreciable amounts of medium Ca^{2+} in the presence of precipitable anions [1]. A typical experiment, using oxalate, is shown in Fig. 2, where free medium [Ca^{2+}], $[Ca^{2+}]_{free}$, was monitored with the fluorescent calcium indicator, Fluo-3. Initial levels were in the range 0.8 to 1.2 μM, whilst total Ca^{2+}, measured by atomic absorption, was 5 to 10 μM. Following preincubation with 100 μM Ca^{2+}, addition of ATP caused a rapid decrease in fluorescence, which is presumed to be mostly due to chelation of Ca^{2+} by ATP, since it is similar to that in the absence of vesicles. Following a delay period, uptake is accelerated to V_{max} due to 'seeding' of intravesicular calcium oxalate crystals [22] Transport ceased abruptly at a characteristic limiting value (F_{lim}), typically in the range equivalent to 100 to 200 nM $[Ca^{2+}]_{free}$. This value has been defined operationally as F_{lim}, from which $[Ca^{2+}]_{lim}$ was calculated according to Eq. 1.

Pulsed additions of Ca^{2+} showed a rapid uptake and return to relatively constant baseline $[Ca^{2+}]_{lim}$. Widths of the peaks were used to give an indication of relative rates of calcium transport under conditions of the assay, and for comparative purposes, the time to reach half maximum fluorescence, $(F_{max}-F_{min})/2$ or $t_{0.5}$, was used as an indication of uptake rate, since transport is assumed to be near V_{max} above the K_d for binding of Ca^{2+} to Fluo-3 (450 nM).

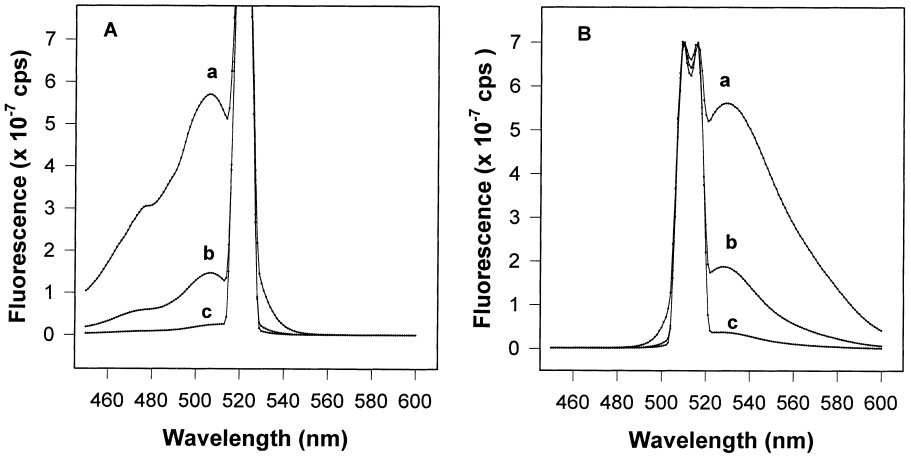

Fig. 1. Fluorescence spectra of Fluo-3. The reaction medium, 2.5 ml at 25°C, contained 20 mM Tris–MOPS (pH 6.8), 5 mM sodium oxalate and 200 nM Fluo-3. Excitation spectra were with 535 nM emission, and emission spectra were with excitation at 509 nM. Excitation (A) and emission (B) spectra were recorded (a) after addition of 100 μM $CaCl_2$, (b) followed by 2.0 mM ATP and further 5 min incubation to reach $[Ca^{2+}]_{lim}$, and (c) following addition of 5 mM EGTA.

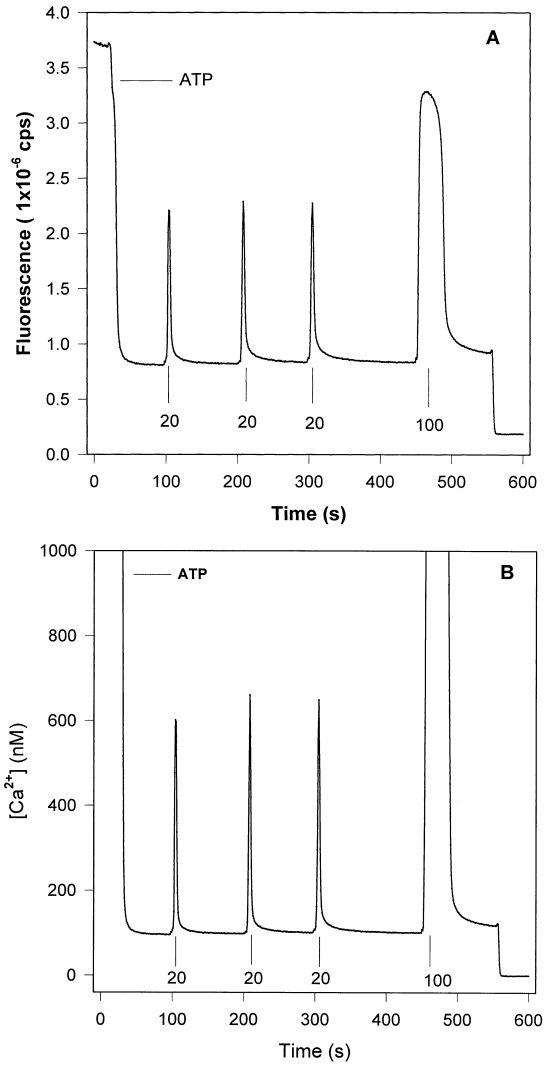

Fig. 2. Kinetics of Ca^{2+} uptake recorded with Fluo-3. SR vesicles, 0.25 mg/ml in standard medium, 2.5 ml, containing 5 mM sodium oxalate, 5 mM $MgCl_2$, and 20 nM Fluo-3, were incubated at 25°C (F_{max}). ATP, 2 mM, was added after 10 s, followed by three aliquots of 20 μM $CaCl_2$ at 100, 200 and 300 s. Ca^{2+}, 100 μM, was added at 450 s, and finally EGTA, 5 mM, was added at 560 s (F_{min}). The limiting fluorescence, F_{lim}, and the corresponding calculated $[Ca^{2+}]_{free}$, $[Ca^{2+}]_{lim}$, was measured immediately before the first addition of Ca^{2+}. Fluorescence readings are shown in A, and their transform to $[Ca^{2+}]_{free}$, using Eq. 1, in B.

Both oxalate and phosphate have previously been used to precipitate intravesicular Ca^{2+} [1,23], and to ensure maximum rates of transport that are not inhibited by internal free Ca^{2+}. The anion dependence of $[Ca^{2+}]_{lim}$ is shown in Fig. 3. Minimum $[Ca^{2+}]_{lim}$ values occurred with 2 to 5 mM oxalate, whereas 10 mM phosphate was still below the optimum concentration. All further experiments were carried out with 5 mM oxalate, since high levels of phosphate might cause inhibition of transport by reversal of the catalytic cycle, especially at low medium free $[Ca^{2+}]$.

The possible contribution of increased light scattering due to accumulation of intravesicular calcium oxalate crystals was considered. Fluorescence at zero $[Ca^{2+}]_{free}$, (F_{min}) was established with 5 mM EGTA after each experiment, and varied in the range 2–5% of F_{max}. Emitted light of vesicles with EGTA, loaded with endogenous Ca^{2+} ($\simeq$ 30 nmol/mg), was 2.9%, and rose to 6.2% of F_{max} following maximum loading of 2000 nmol/mg. The positive error in estimation of $[Ca^{2+}]_{lim}$ in a typical experiment was calculated to be equivalent to 0.12 nM, or 0.15% of F_{max}. It can be concluded, therefore, that light scattering does not contribute significantly to emitted light at $[Ca^{2+}]_{lim}$.

Feher and Lipford [23] have studied the factors limiting maximum calcium oxalate loading of 4–6 μmol/mg SR, and have concluded that the rate limiting process is due to rupture of vesicles. Loading in the present study was limited to 1 μmol/mg and showed no increase of $[Ca^{2+}]_{lim}$ with multiple pulsed

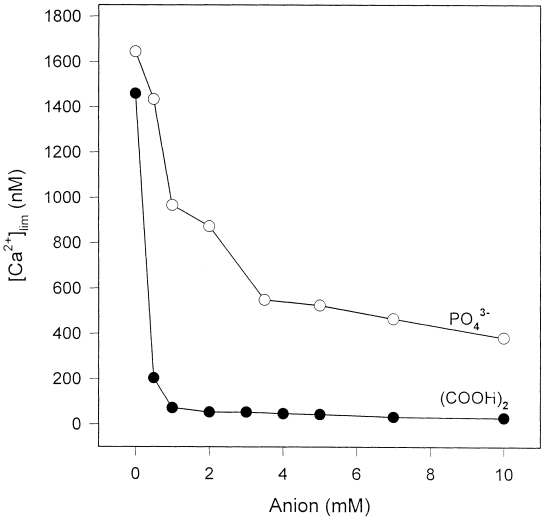

Fig. 3. Oxalate and phosphate dependence of $[Ca^{2+}]_{lim}$. Standard conditions were as described in Fig. 2, except that oxalate was omitted and 20 mM histidine added (see below). SR vesicles were preincubated with 20 μM Ca^{2+} and varying concentrations of sodium oxalate or NaH_2PO_4. Following addition of 2 mM ATP, fluorescence was recorded for 100 s, when F_{lim} was measured and $[Ca^{2+}]_{lim}$ calculated.

additions of Ca^{2+} within this range. It is therefore concluded that saturation of loading capacity is not the cause of the inability of the SR to decrease $[Ca^{2+}]_{free}$ below $[Ca^{2+}]_{lim}$. The electrochemical potential, $\Delta\Psi$, is also presumed to be minimal in SR due to an active anion channel [24].

The free energy of hydrolysis of ATP does not appear to be fully realised for sustaining a Ca^{2+} gradient in the presence of oxalate. Following addition of 2 mM ATP and transport of 100 μM Ca^{2+}, which, assuming tight coupling, would result in hydrolysis of 50 μM ATP, the concentration quotient [ATP]/[ADP][P_i] is 7.8×10^5 M^{-1}. Assuming that the free energy available from ATP hydrolysis is 14 kcal/mol [25], this will be in equilibrium with a transmembrane gradient of 10 000:1 [12]. Since intravesicular free $[Ca^{2+}]$ in oxalate-loaded vesicles is in the range 5–10 μM, at equilibrium extravesicular levels are expected in the range 0.5 to 1 nM. Observed $[Ca^{2+}]_{lim}$, calculated from the lowest fluorescence signal from Fluo-3, of 100 to 200 nM, is at least two orders of magnitude higher.

Several mechanisms for spuriously high fluorescence at $[Ca^{2+}]_{lim}$ are possible. Calculation of free $[Ca^{2+}]$, based on Eq. 1, assumes a single pool of fluophore. Mg^{2+} also forms a fluorescent complex with Fluo-3. The K_d for Mg^{2+} binding is 9 mM at 25°C [18]. Binding of Mg^{2+} is probably to a site on Fluo-3 that is remote from the chromophore since the Mg^{2+}–Fluo-3 complex is only 1.4-fold more fluorescent than the free fluophore, compared to the 40-fold enhancement following Ca^{2+} binding. Free Mg^{2+} is not expected to vary during the course of usual experimental protocols, and would not be quenched by EGTA. Hence the presence of Mg^{2+} in the medium, or in vivo in cytoplasm, should not affect calibration of the Fluo-3 signal.

3.2. Contribution of Zn^{2+} to F_{lim}

The characteristics of residual fluorescence of Fluo-3 at $[Ca^{2+}]_{lim}$ are that it is resistant to active uptake of Ca^{2+} into vesicles, and that it is quenched to a large extent by EGTA (F_{min}) to levels of 5–8% of F_{max} with excess Ca^{2+}. This suggested possible contamination by transition elements, which are known to form stable complexes with Fluo-3. Zn^{2+} is such a possible contaminant and is one of the most abundant divalent cations in the cytosol of cells, including muscle [26]. Varying SR concentration in the range 0.05 to 0.25 mg/ml did not affect F_{lim} in the absence of histidine (data not shown). Zn^{2+} is known to bind to Fluo-3 more tightly than Ca^{2+} with a K_d of approx. 1.5 nM [18]. The Zn^{2+} complex is 61% as fluorescent as the Ca^{2+} complex, and therefore saturation with Zn^{2+} is equivalent to a $[Ca^{2+}]$ of 680 nM.

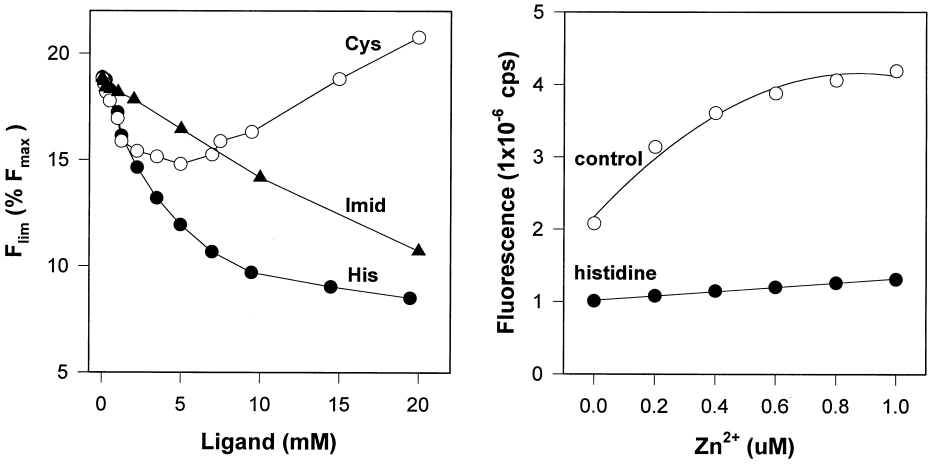

Fig. 4. Effects of histidine, imidazole and cysteine on F_{lim}. SR vesicles, 0.25 mg/ml, were preincubated with 100 μM Ca^{2+} at 25°C. ATP, 2 mM, was added, and following 100 s, $[Ca^{2+}]_{lim}$ was calculated. In A, increasing concentrations of histidine or cysteine were added and F_{lim} recorded. Titration of a medium mixture at $[Ca^{2+}]_{lim}$ with added Zn^{2+}, with and without histidine is shown in B. Following establishment of steady state of F_{lim}, 100 s after addition of 2 mM ATP, increasing amounts of $ZnCl_2$ were added and the increase in fluorescence intensity was recorded, with and without 20 mM histidine.

The effects of Zn^{2+} ligands histidine, imidazole and cysteine on Fluo-3 fluorescence at $[Ca^{2+}]_{lim}$ are shown in Fig. 4A. Histidine decreased F_{lim} from 20% of F_{max} to 8% with $K_{0.5}$ of 3 mM. Imidazole was less effective, with a linear decrease up to 20 mM, with no signs of saturation. Cysteine was somewhat anomalous in that in the 0 to 5 mM range it had similar effects to those of histidine, but the decrease was reversed and even increased to above the zero value at 20 mM ligand. Addition of $ZnCl_2$ confirmed that the Zn^{2+} complex of Fluo-3 is stable and fluorescent, and that fluorescence is quenched by histidine (Fig. 4B). Extrapolation of Zn^{2+} titration of fluorescence effects of suspensions of SR vesicles in the assay medium indicate a Zn^{2+} content of 1.3 nmol/mg.

Direct analysis of four concentrated SR vesicles suspensions for Zn^{2+} by atomic absorption spectrophotometry gave values of 0.47 ± 0.04 nmol/mg protein, which are comparable to that found by Szabolcs [27]. Presumably the higher Zn^{2+} content of SR vesicles suspended in the incubation medium represents contributions from its components. On the basis of these findings, all further studies were carried out on suspensions of vesicles to which 20 mM histidine was added in addition to Tris–MOPS buffer at pH 6.8. Profiles of Ca^{2+} additions to actively transporting SR vesicles, with and without 20 mM histidine or 2 μM Zn^{2+} are shown in Fig. 5. Histidine decreased $[Ca^{2+}]_{lim}$, resulting in a value for $[Ca^{2+}]_{lim}$ of 49 ± 1.8 nM ($n = 12$).

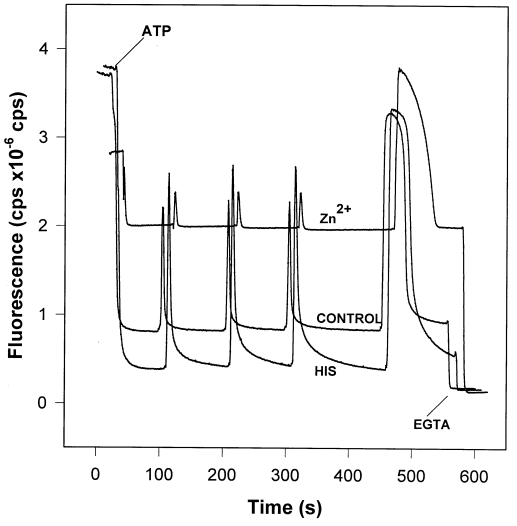

Fig. 5. Effects of histidine and Zn^{2+} on the kinetics of Ca^{2+} uptake and on limiting fluorescence, F_{lim}. SR vesicles, 0.25 mg/ml, were incubated with standard buffer (control), or with 20 mM histidine, or 2 μM zinc acetate. Following addition of 2 mM ATP, three 20-μM pulses of Ca^{2+} were added at 100, 200 and 300 s, 100 μM Ca^{2+} at 450 s and 5 mM EGTA at 480 s. Traces have been offset by 10 and 20 s on the x-axis for clarity.

3.3. Free calcium ion concentration dependence of Ca^{2+} transport in the absence of EGTA

Previous studies aimed at determining the $[Ca^{2+}]$-dependence of transport have relied on Ca/EGTA buffering systems to clamp extravesicular $[Ca^{2+}]$, and have used $^{45}Ca^{2+}$ as tracer [2]. The present experimental system suggests an alternate approach where, following depletion of medium Ca^{2+}, a constant infusion of $CaCl_2$ would lead to a rise in medium Ca^{2+} and to a new steady state, at which rates of infusion and active transport are balanced at a defined $[Ca^{2+}]$. Typical traces, with three constant infusion rates, are shown in Fig. 6A. An initial lag phase of 10–20 s after infusion commenced is presumed to be inertia of the infusion system and washout of the infusion tip. Flow rates were typically in the range of 10–100 μl/min. Total times to reach plateau phase were 10–30 s. For low infusion rates the plateau phase was stable for up to 100 s. At higher rates there was a slow rise, termed a pseudo-steady state, since there was a slow increase of $[Ca^{2+}]_{free}$ during this phase. This rise is not due to failure to reach a balance between infusion and active uptake rates since $[Ca^{2+}]_{free}$ declined rapidly and returned to the steady state when the infusion was switched off and on again (see inset to Fig. 6A). The slow rise is presumed to be due to filling of a subpopulation of vesicles. Initial steady state levels of $[Ca^{2+}]_{free}$ were obtained by linear extrapolation to zero infusion time, which was taken as the beginning of the rise from $[Ca^{2+}]_{lim}$.

The constant infusion system for determining Ca^{2+}-dependence of transport reverses the usual methods, where $[Ca^{2+}]_{free}$, set by Ca/EGTA buffers, is fixed as the independent variable, and transport, measured at varying $[Ca^{2+}]$, is the dependent variable. In the constant infusion method, fixed infusion rates are equivalent to transport, and are plotted on the y-axis. The data are plotted in Fig. 6B, with

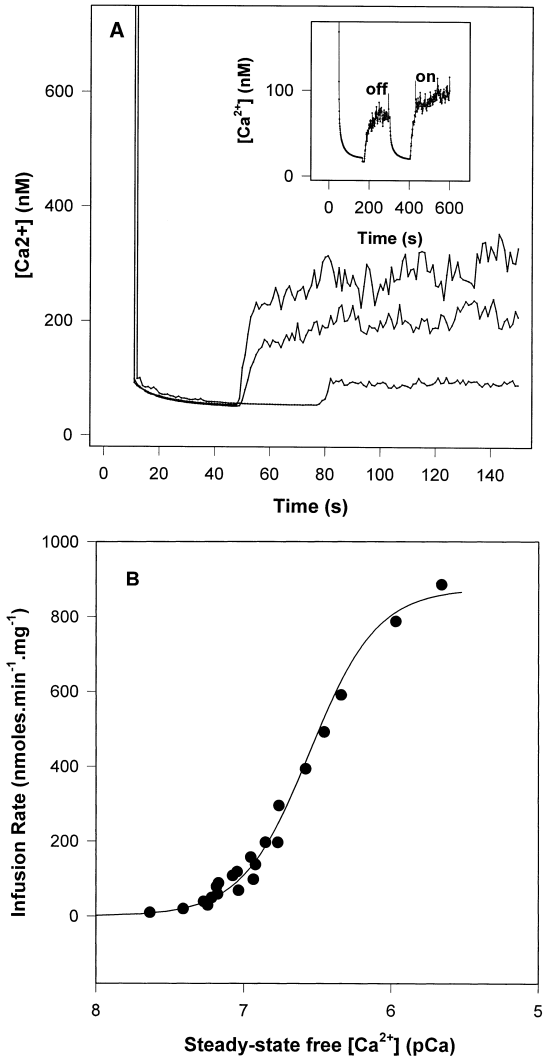

Fig. 6. Determination of the Ca^{2+}-dependence of transport by the constant infusion method in the absence of Ca^{2+}-chelators. SR vesicles were preincubated with 5 mM sodium oxalate, 20 mM histidine, 20 nM Fluo-3 and 100 μM $CaCl_2$. ATP, 2 mM, was added, and following a delay for attaining the steady state of $[Ca^{2+}]_{lim}$, a constant infusion of 5 mM standardised $CaCl_2$ was begun with continuous stirring. The effects of stopping and starting the infusion pump are shown in the inset to A. The $[Ca^{2+}]$ at which active transport matched infusion rates were estimated from linear extrapolation of the plateau phase back to t_0, the time at which $[Ca^{2+}]$ rose above $[Ca^{2+}]_{lim}$ at the start of infusion. Three examples at rates of infusion of (a) 157, (b) 98.4 and (c) 19.6 nmol Ca^{2+}/mg per min are shown in A. Many more rates of infusion and matched levels of $[Ca^{2+}]$ were used to construct the plot showing the $[Ca^{2+}]$-dependence of transport in B. The continuous curve is for $V_{max} = 853$ nmol/min per mg, $K_{0.5} = 279$ nM, and $n_{H(Ca)} = 1.89$.

steady-state $[Ca^{2+}]$ and infusion rates as independent and dependent variables, respectively. Rates of Ca^{2+} uptake are generally considered to be tightly coupled to ATP hydrolysis in the presence of oxalate, with $K_{0.5}$ in the range 0.1 to 2.0 μM, mainly due to the use of varying values for the dissociation constant of CaEGTA, and $n_{H(Ca)}$ in the range 1.6 to 2.0 [2]. The data for the $[Ca^{2+}]$-dependence of transport in Fig. 6B were fitted by non-linear regression, assuming (a) that there is no leak, and (b) that $n_{H(Ca)}$ is fixed. The best-fit curve is for $V_{max} = 853$ nmol/min per mg, $K_{0.5} = 279$ nM, and $n_{H(Ca)} = 1.89$. These values are in good agreement with those obtained with $^{45}Ca^{2+}$ and Ca/EGTA buffers [3]. The nature of the constant infusion method is that data are best obtained up to 3–4 times the K_d of the indicator, i.e., 1.5–2.0 μM, which also coincides with the range of up to 5-fold that of the $K_{0.5}$ for transport.

3.4. *Effects of varying V_{max} with temperature, pH and alternate substrates on $[Ca^{2+}]_{lim}$*

Under physiological conditions the Ca-ATPase operates at near equilibrium [12]. Possible mechanisms for the observed higher than predicted $[Ca^{2+}]_{lim}$ in vitro were explored. This behaviour may be an intrinsic feature of the Ca^{2+} pump, or a kinetic barrier, such that medium free Ca^{2+} cannot be decreased below 35 to 45 nM. Alternatively it may represent a steady state in which either active transport balances reversal of the pump mechanism, or that it is a manifestation of steady state cycling between active uptake and non-specific passive leakage pathways. For the latter mechanism it is expected that $[Ca^{2+}]_{lim}$ would be sensitive to conditions which affect Ca^{2+} pump activity.

Temperature and pH changes were varied to modulate Ca^{2+}-ATPase turnover. Their effects on V_{max} of transport and on the levels of $[Ca^{2+}]_{lim}$, are shown in Fig. 7. In the range 10–37°C transport varied >500-fold. $[Ca^{2+}]_{lim}$ was relatively constant between 30 and 50 nM over the range 15–40°C. Similarly, pH changes had relatively little effect on $[Ca^{2+}]_{lim}$, which was constant between pH 6 and 8, when maximum transport activity varied 10-fold.

Alternate substrates can support Ca^{2+} transport at widely varying rates. Traces of uptake of Ca^{2+}, when supported by ATP, AcP and by *p*-NPP, are shown in

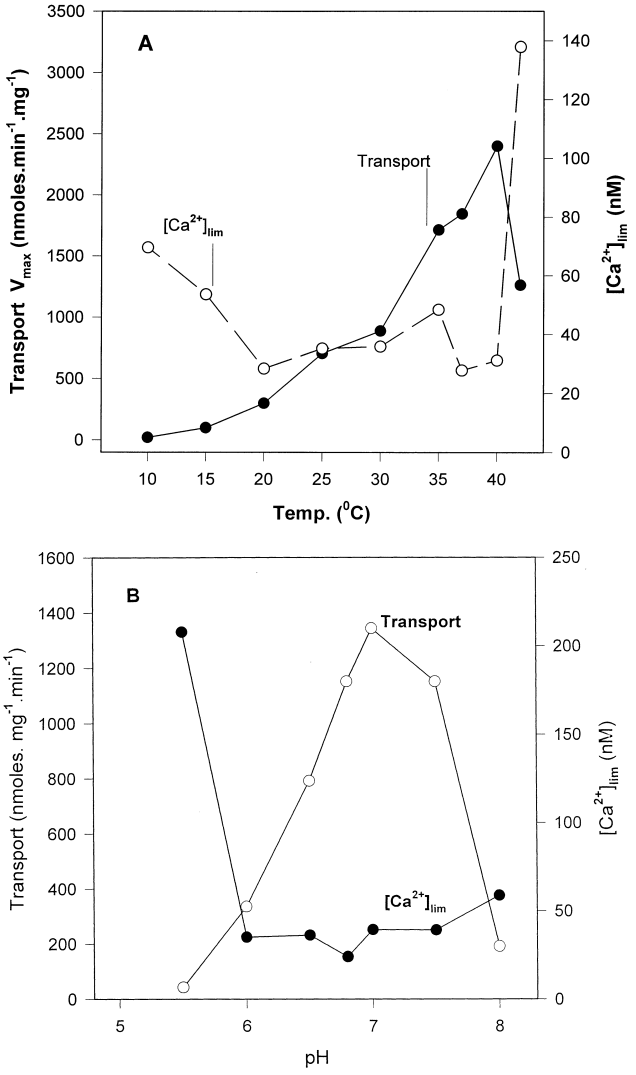

Fig. 7. Effects of temperature and pH on V_{max} of Ca^{2+} transport and on $[Ca^{2+}]_{lim}$. SR vesicles were suspended in standard buffer, containing 20 μM Ca^{2+} and 20 mM histidine at varying temperatures (A), and at constant temperature of 25°C and varying pH in (B). $[Ca^{2+}]_{lim}$ was taken from the minimum fluorescence value after addition of ATP. Maximum transport rates were calculated from the widths of peaks following addition of 100 μM, as described in Section 2.

Fig. 8. Rates of transport with AcP and *p*-NPP are approximately one and two orders slower than with ATP, nevertheless final $[Ca^{2+}]_{lim}$ values with *p*-NPP were lower than with the natural substrate. Fluorescence excitation and emission spectra taken at $[Ca^{2+}]_{lim}$ were similar for all three substrates (data not shown). It may be concluded that changes in temperature, pH and substrate, which vary V_{max} of transport over a wide range, have little effect on the steady state levels of Ca^{2+} at $[Ca^{2+}]_{lim}$.

3.5. *Estimation of the magnitude of leakage pathways at $[Ca^{2+}]_{lim}$*

It can be assumed that at the steady state, characterised as $[Ca^{2+}]_{lim}$, active transport is balanced by efflux from SR vesicles. Efflux pathways from SR vesicles in the absence of precipitable anions, and consequent high millimolar $[Ca^{2+}]_{in}$, are divided roughly equally between back inhibition or reversal of the pump cycle, slippage or turnover in the absence of a transport cycle, and passive efflux through the SR membrane independent of the Ca^{2+}-ATPase [17]. An estimate of the magnitude of total efflux of Ca^{2+} can be obtained from the unidirectional inward flux, as estimated with $^{45}Ca^{2+}$, during steady state, and is shown in Fig. 9. Addition of tracer to the medium at $[Ca^{2+}]_{lim}$ resulted in finite binding to SR at time zero (10 s), which explains initial levels of 1.7 nmol/mg when tracer is in rapid equilibrium with high affinity transport sites. Further slow exchange is due to unidirectional inward flux of Ca^{2+}, and was calculated from the initial slope at t_0 to be 0.19 nmol/

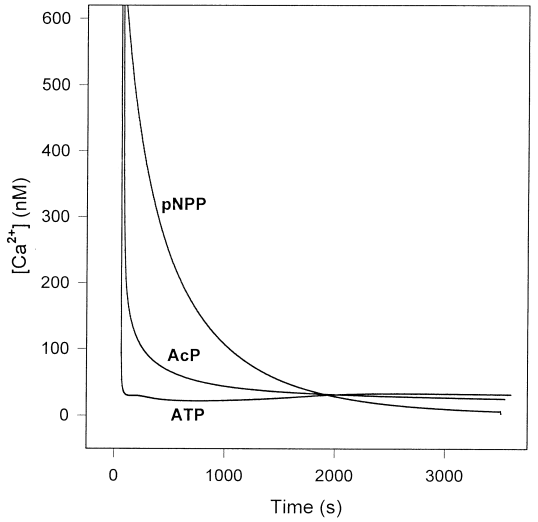

Fig. 8. Kinetics of Ca^{2+} transport and $[Ca^{2+}]_{lim}$ values with ATP and pseudosubstrates, acetyl phosphate and *p*-NPP. SR vesicles, 0.25 mg/ml were suspended in buffer at pH 6.8 and 25°C, containing 20 mM histidine, 5 mM oxalate, 20 μM Ca^{2+} and 20 nM Fluo-3. Substrates, added at $t = 15$ s, were 5 mM ATP, 5 mM acetyl phosphate (AcP) or 10 mM *p*-NPP. EGTA, 5 mM, was added at $t = 3550$ s.

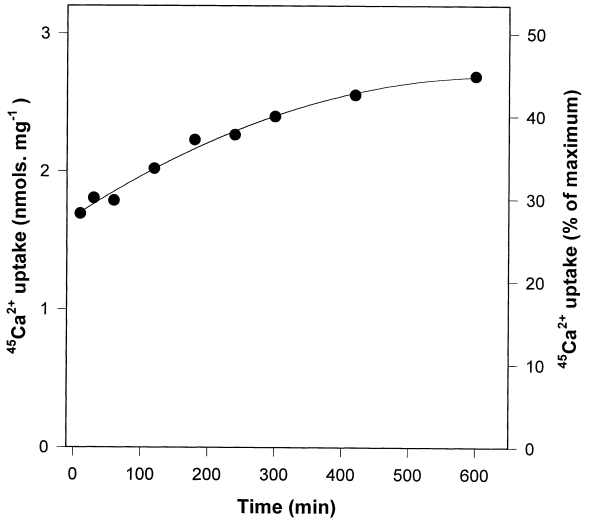

Fig. 9. Exchange of $^{45}Ca^{2+}$ into SR vesicles, preloaded with ^{40}Ca. Oxalate, at $[Ca^{2+}]_{lim}$. SR vesicles, 0.25 mg/ml, were actively preloaded with 2 mM ATP and 400 nmol/mg $^{40}Ca^{2+}$. Following achievement of $[Ca^{2+}]_{lim}$ after 5 min, 0.1 μCi/ml $^{45}CaCl_2$ was added at time zero. Samples, 0.1 ml, were taken first at 10 s and at timed intervals, filtered onto Millipore 0.45-μm filters, and washed with medium containing 10 mM $^{40}CaCl_2$. Uptake of Ca^{2+} was calculated assuming medium free $[Ca^{2+}]$ of 100 nM. Total extravesicular Ca^{2+} was assumed to be 1.5 μM based on 15-fold buffering,as determined from titration of SR vesicles at $[Ca^{2+}]_{lim}$ with Ca^{2+} following inhibition of uptake with 5 μM thapsigargin. The initial rate of uptake at zero time was calculated to be 0.19 nmol/mg per min from the slope of the second-order fitted curve.

mg/min, or 0.02% of V_{max}. Near maximum equilibration of approx. half of total $^{45}Ca^{2+}$ occurred after 10 min.

Leakage was also estimated from efflux at $[Ca^{2+}]_{lim}$ following depletion of substrate, ATP. A typical experiment is shown in the inset to Fig. 10. ATP, 0.25 mg, was added, following preincubation with 100 μM Ca^{2+}. Following uptake of this pulse of Ca^{2+}, it is presumed that 0.2 mM ATP remains. This was depleted within 70 min at 25°C, following which near linear efflux occurred. Rates of efflux and their temperature dependence are shown in Fig. 10. Efflux at 25°C, the temperature at which $[Ca^{2+}]_{lim}$ was usually monitored, was 2.8 nmol/min per mg, i.e., 0.3% of V_{max} of transport. It is possible that efflux pathways are greater during active uptake due to a non-equilibrium state of intravesicular Ca^{2+} stores [22,23,28]. This is supported by higher ATPase activity in the presence of ionophore A23187 than with oxalate [29]. However, this cannot explain the steady state of $[Ca^{2+}]_{lim}$, which was stable for up to 12 h, provided that sufficient ATP is present to sustain the slow turnover rate (data not shown). It is presumed, therefore, that at $[Ca^{2+}]_{lim}$ internal $[Ca^{2+}]_{free}$ is in equilibrium with oxalate bound species, and is of the order of 10 μM [1]

4. Discussion

This study demonstrates the usefulness of Fluo-3 as a fluophore for determining extravesicular $[Ca^{2+}]_{free}$ in suspensions of SR vesicles. Excitation and emission spectra are in the visible range, which obviates autofluorescence from cofactors, such as NADH, or from protein arising from tryptophan residues. Another major advantage is that because of the 40-fold increase in fluorescence on binding of Ca^{2+}, nanomolar quantities of Fluo-3 give excellent signal to noise ratios, and it should be possible to conduct studies in vitro at less than 20 nM, whilst

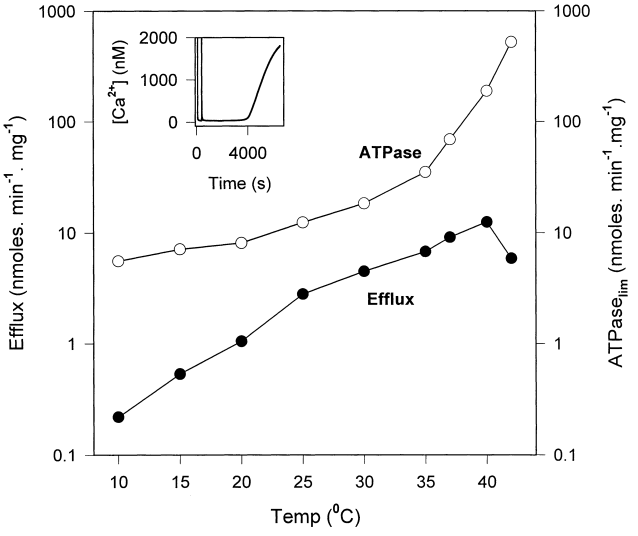

Fig. 10. Effects of temperature on Ca^{2+} efflux from actively loaded SR following depletion of substrate. SR vesicles, 0.25 mg/ml in histidine 20 mM, were actively loaded with 100 μM $CaCl_2$ and 0.25 mM ATP. A typical efflux curve is shown in the inset. Maximum rates of efflux were calculated from the slopes of the $[Ca^{2+}]$ curve following depletion of ATP, and from buffering in the medium of 15-fold, described in Fig. 9. Comparative rates of ATPase activity during the prolonged steady state were determined from the delay between the initial transient and the beginning of the efflux phase.

the Ca^{2+}-ATPase totals 1 μM (0.25 mg/ml at 4 nmol/mg). The K_d for Ca^{2+} binding to Fluo-3 (~400 nM) is similar to the $K_{0.5}$ for Ca^{2+} binding to the Ca^{2+}-ATPase (~250 nM). For comparison, 20 μM Arsenazo III has been shown to interact with SR vesicles, causing optical artefacts, as well as near 3-fold inhibition of transport and ATPase activity [30]. Furaptra, a 'tricarboxylate' calcium chromophore, has been shown to bind to myoplasmic constituents in vivo [31]. Similarly, Indo-1, used to establish resting intracellular $[Ca^{2+}]_i$ in cardiac myocytes, shows decreased affinity for Ca^{2+} that has been related to protein binding [32]

Initially we used Tris–MOPS buffers and noted that following prolonged incubation of SR in the presence of oxalate and excess ATP, the steady-state fluorescence of Fluo-3, F_{lim}, was equivalent to 100 to 200 nM Ca^{2+}. Possible errors in determining $[Ca^{2+}]_{lim}$ were investigated. The nature of the fluorescence at $[Ca^{2+}]_{lim}$ is that it is the minimum fluorescence signal following transport of Ca^{2+} into SR vesicles and that is quenched by EGTA. Papp et al. [26] have determined the transitional element content of SR preparations and media used for assay of the reaction of the Ca^{2+}-ATPase with *N*-(1-pyrene)maleimide, and have suggested that Zn^{2+} may regulate SH reactivity. This represents interaction with a subpopulation of pump units, since the Zn^{2+} content, as measured by plasma emission spectroscopy, was 0.75 nmol/mg or 0.19 mol per mol ATPase.

The possibility that Zn^{2+} might be responsible for the falsely raised F_{lim} in the present study was investigated, since Zn^{2+} is known to bind with high affinity to Fluo-3, and for the adduct to be fluorescent [18]. The effects of known ligands, histidine, imidazole and cysteine (Fig. 4) are consistent with the idea that Zn^{2+} may contribute to F_{lim}. Furthermore, addition of Zn^{2+} can reverse the effects of histidine. Cysteine effects were anomalous, in that submicromolar concentrations quench F_{lim}, similar to the action of histidine on a mol per mol basis, but higher concentrations increase F_{lim} to levels greater than controls. Cysteine has been shown to interact with the Ca^{2+}-ATPase, altering its conformation, as shown by tryptophan autofluorescence [33]. Added Zn^{2+} was shown to increase F_{lim}, and the calculated contribution to F was such that the endogenous content of SR plus media is by extrapolation equivalent to 247 nM Zn^{2+}, i.e., 1.0 nmol/mg. By comparison, direct assay gave a value of 0.49 nmol/mg. It appears that SR vesicles and the medium contribute equally to the Zn^{2+} content of the experimental system.

Several previous studies have shown evidence for interaction of Zn^{2+} with components of SR membranes. Papp et al. [26] have determined Zn^{2+} content of native and water washed SR microsomes at 0.75 to 1.35 nmol/mg, about 30% of which is removed by EGTA or Chelex treatment. Alterations in Zn^{2+} content could be correlated with SH reactivity. Picello et al. [34] have found that the histidine-rich Ca^{2+}-binding protein, located in junctional membranes of rabbit skeletal muscle, has independent low-affinity Ca^{2+} binding sites and high-affinity Zn^{2+} sites that are inhibited by prior reductive alkylation. Phosphorylation of phospholamban of cardiac muscle is decreased by micromolar Zn^{2+} due to inhibition of endogenous Ca^{2+}/calmodulin-dependent kinases, whilst millimolar concentrations inhibit Ca^{2+}-independent autophosphorylation [35].

The experimental approach employed in this study was aimed at characterising calcium transport by isolated SR vesicles at concentrations of medium free Ca^{2+} that are limiting for uptake. Limiting $[Ca^{2+}]$ was achieved in the absence of chelating agents generally employed to buffer medium $[Ca^{2+}]$, by translocation of medium Ca^{2+} into SR vesicles. The use of oxalate as a precipitable anion ensured that intravesicular $[Ca^{2+}]$ was clamped in the 5 to 10 μM range, which minimises back inhibition of the transport cycle, and that the transmembrane gradient was of the order of 100:1. This condition is designated as 'free flow' in terms of irreversible thermodynamics, since the gradient is lower than could be achieved at thermodynamic equilibrium, whose calculated value at $[Ca^{2+}]_{lim}$, assuming tight coupling, 10% hydrolysis of 2 mM ATP ($\Delta G = -55.6$ kJ/mol) and $[Ca^{2+}]_{in} = 10$ μM, is 0.14 nM, i.e., more than two orders lower than that measured. Erythrocyte Na^+,K^+-ATPase is not in equilibrium with cytosolic phosphorylation potential, as determined by ^{31}P-NMR [36].

Passive leaks of Ca^{2+} could explain higher than expected $[Ca^{2+}]_{lim}$, as originally suggested by Gatass and de Meis [37]. Measured efflux rates following substrate ATP depletion were at least two orders slower than V_{max} of transport, suggesting that passive leakage cannot explain the anomalous $[Ca^{2+}]_{lim}$.

Gerdes and Moller [28] have studied the Ca^{2+} permeability of SR vesicles, both in the energised and non-energised states. They have concluded that efflux is activated, and possibly coupled to active influx, and have suggested that is involves the partial reaction $2Ca^{2+}_{in}+E_2 \leftrightarrow E_2 2Ca \leftrightarrow E_1+2Ca^{2+}_{out}$. Since activated efflux and passive outflow are reciprocally related, they have also suggested that the two processes involve a common membrane channel. Although in the present study efflux is expected to be enhanced during active uptake at high $[Ca^{2+}]_{out}$, the slow passive outflow at $[Ca^{2+}]_{lim}$ is insufficient to explain failure to reach thermodynamic equilibrium.

A prediction of the pump/leak model is that $[Ca^{2+}]_{lim}$ would be expected to vary with changes in transport rate. The data obtained here show that when transport rates are varied with changes in pH and temperature, $[Ca^{2+}]_{lim}$ remained relatively constant. Perhaps most compelling evidence against the pump/leak model is the relative constant value for $[Ca^{2+}]_{lim}$ with various substrates, whose V_{max} varied some 500-fold. Paradoxically, the lowest activity substrate, *p*-NPP, appeared to be the most thermodynamically efficient. One possibility considered was that reversal of the pump with accumulation of ADP, with ATP as substrate, might predispose to higher levels of $[Ca^{2+}]_{lim}$. However, with acetyl phosphate, where there is no possibility of reversal, $[Ca^{2+}]_{lim}$ was similar to that with ATP.

In their original study on the effect of $[Ca^{2+}]$ on calcium uptake, Weber et al. [13], using Ca/EGTA buffers, found significant transport activity at resting muscle levels of calcium (100 nM), which were approx. 30% of that measured at saturating $[Ca^{2+}]$ (1 μM). In addition the ratios of uptake to ATP hydrolysis that approached 2.0 did not change between 30 to 100 nM $[Ca^{2+}]$. The close agreement between $[Ca^{2+}]$-dependencies of binding and of transport has previously been interpreted as support for tight coupling and high thermodynamic efficiency. We have previously shown significant effects of EGTA, presumed to be due to the species CaEGTA, on transport rates in the sub-micromolar Ca^{2+} range [38]. Combettes et al. [39] have also found anomalous effects of calcium chelators in their studies on the effects of IP_3-induced Ca^{2+} release from cerebellar microsomes, where the inhibitory effect appeared to be due to metal-free chelator. Activation of lymphocyte plasma membrane Na^+/K^+-ATPase is better explained by chelation of Zn^{2+} rather than by calcium chelation [40]. We now confirm that Ca^{2+} dependence of transport is similar in the absence of chelator with previous findings in their presence. Previously described effects of chelators can only be implicated if they occur at higher levels than those in reagents and tissue preparations.

Our current understanding of the possible role of chelators or their Ca^{2+}-complexes is (a) that the kinetics of the Ca^{2+}-dependence of transport are similar when determined with or without chelators, (b) that contaminating Zn^{2+} interferes with calibration of Fluo-3 determination of free $[Ca^{2+}]$, (c) that this problem can be minimised with a histidine buffer, and (d) that Zn^{2+} cannot contribute to modified behaviour of the Ca^{2+}-ATPase since it occurs in substoichiometric amounts (approx. 0.1 mol per mol ATPase).

A practical issue, arising from the present study, and relevant for calibration of intracellular Ca^{2+} levels in vivo, is that binding of Zn^{2+} to Ca^{2+} fluophores might enhance fluorescence, especially in the resting state. Since EGTA quenches both Ca^{2+}- and Zn^{2+}-fluophore signals, histidine buffers may be used in these circumstances to minimise overestimation of cytoplasmic $[Ca^{2+}]_{free}$.

The phenomenon of a non-equilibrium value for $[Ca^{2+}]_{lim}$ in the resting muscle cell, and the possibility that this may be an intrinsic property of the SR calcium pump, have interesting physiological implications. On the basis of occupancy of binding sites from well-characterised Ca^{2+} binding parameters, it can be calculated that under resting or relaxed muscle conditions (approx. 100 nM cytosolic free Ca^{2+}), ATP hydrolysis by SR should be approx 2% of maximum. Assuming V_{max} at 37°C of 10 μmol/mg per min [41], and skeletal muscle SR content of 52 mg/g muscle protein [42], it can be estimated that turnover of the Ca^{2+}-ATPase of skeletal SR in the relaxed state could contribute 10% to 15% of basal metabolism. Simonides and van Hardeveld [43] have estimated the ATPase activity required by SR to maintain the Ca^{2+} gradient, and have calculated that this may account for 20% of the resting metabolic rate in skeletal muscle. Although these figures have a degree of uncertainty, it seems reasonable to suggest, based on the evidence presented here and

elsewhere, that skeletal SR can contribute significantly to overall basal metabolism in mammals as a kind of Ca^{2+}-regulated heat organ. De Meis et al.[44,45] have recently measured heat production directly during uncoupled Ca^{2+} efflux, confirming that SR is a major source in animals and humans in non-shivering thermogenesis.

Acknowledgements

This work was supported by grants from the South African Foundation for Research and Development, the South African Medical Research Council, and from the Harry Crossley and Staff Research Funds of the University of Cape Town. I am indebted to Abduraman Mohammed for excellent technical assistance, to Prof. David McIntosh for stimulating discussions and suggestions, and to the South African Medical Research Council, the University of Cape Town Staff Research Fund, and the Harry Crossley Foundation for financial support.

References

[1] W. Hasselbach, Top. Curr. Chem. 78 (1979) 1–56.
[2] L. De Meis, The Sarcoplasmic Reticulum: Transport and Energy Transduction, John Wiley and Sons, New York, 1981.
[3] G. Inesi, Annu. Rev. Physiol. 47 (1985) 573–601.
[4] H.J. Schatzmann, Annu. Rev. Physiol. 51 (1989) 473–485.
[5] G. Inesi, C. Sumbilla, M.E. Kirtley, Physiol. Rev. 70 (1990) 749–760.
[6] M.C. Berman, Biochim. Biophys. Acta 694 (1982) 95–121.
[7] V. Forge, E. Mintz, F. Guillain, J. Biol. Chem. 268 (1993) 10953–10960.
[8] W.P. Jencks, J. Biol. Chem. 264 (1989) 18855–18858.
[9] J.P. Andersen, Biochim. Biophys. Acta 988 (1989) 47–72.
[10] G. Inesi, J. Biol. Chem. 262 (1987) 16338–16342.
[11] L. De Meis, A.L. Vianna, Annu. Rev. Biochem. 48 (1979) 275–292.
[12] C. Tanford, J. Gen. Physiol. 77 (1981) 223–229.
[13] A. Weber, R. Herz, I. Reiss, Biochem Z. 345 (1966) 329–369.
[14] M.C. Berman, J. Biol. Chem. 257 (1982) 1953–1957.
[15] M.G. Klein, L. Kovacs, B.J. Simon, M.F. Schneider, J. Physiol. 414 (1991) 639–671.
[16] S. Meltzer, M.C. Berman, J. Biol. Chem. 259 (1984) 4244–4253.
[17] G. Inesi, L. De Meis, J. Biol. Chem. 264 (1989) 5929–5936.
[18] A. Minta, J.P. Kao, R.J. Tsien, J. Biol. Chem. 264 (1989) 8171–8178.
[19] P. Champeil, F. Guillain, C. Venien, M.P. Gingold, Biochemistry 24 (1985) 69–81.
[20] D. Ross, G.A. Davidson, D.B. McIntosh, J. Biol. Chem. 266 (1991) 4613–4621.
[21] J.E. Merritt, S.A. McCarthy, M.P.A. Davies, K. Moores, Biochem. J. 269 (1990) 513–519.
[22] V.M.C. Madeira, Biochim. Biophys. Acta 769 (1984) 284–290.
[23] J.J. Feher, G.B. Lipford, Biochim. Biophys. Acta 818 (1985) 373–385.
[24] W. Hasselbach, H. Oetliker, Ann. NY Acad. Sci. 402 (1983) 459–469.
[25] R.L. Veech, W.R. Lawson, N.W. Cornell, H.A. Krebs, J. Biol. Chem. 254 (1979) 6538–6547.
[26] S. Papp, M. Rutzke, A. Martonosi, Arch. Biochem. Biophys. 243 (1985) 254–263.
[27] M. Szabolcs, Acta Biochim. Biophys. Hung. 25 (1990) 111–124. (Abstract)
[28] U. Gerdes, J.V. Moller, Biochim. Biophys. Acta 734 (1983) 191–200.
[29] S. Verjovski-Almeida, G. Inesi, J. Biol. Chem. 254 (1979) 18–21.
[30] S. Riollet, P. Champeil, Anal. Biochem. 162 (1987) 160–162.
[31] M. Konishi, S. Hollingworth, A.B. Harkins, S.M. Baylor, J. Gen. Physiol. 97 (1991) 271–301.
[32] J.W.M. Bassani, R.A. Bassani, D.M. Bers, Biophys. J. 68 (1995) 1453–1460.
[33] Y.P. Tu, F.Y. Yang, Biosci. Rep. 14 (1994) 309–317.
[34] E. Picello, E. Damiani, A. Margreth, Biochem. Biophys. Res. Commun. 186 (1992) 659–667.
[35] L.G. Baltas, P. Karczewski, E.G. Krause, Biochem. Biophys. Res. Commun. 232 (1997) 394–397.
[36] A. Petersen, E.J. Pedersen, B. Quistorff, Biochim. Biophys. Acta 1012 (1989) 267–271.
[37] C.R. Gattass, L. De Meis, Biochim. Biophys. Acta 389 (1976) 506–515.
[38] M.C. Berman, J. Biol. Chem. 257 (1982) 1953–1957.
[39] L. Combettes, Z. Hannaert-Merah, J. Coquil, C. Rousseau, M. Claret, S. Swillene, P. Champeil, J. Biol. Chem. 269 (1994) 17561–17571.
[40] G.B. Segel, W. Simon, A.H. Lichtman, M.A. Lichtman, J. Biol. Chem. 256 (1981) 6629–6632.
[41] W.L. Dean, C. Tanford, Biochemistry 17 (1978) 1683.
[42] E. Leberer, H. Reichmann, J. Neural. Transm. 95 (1994) 29–38.
[43] W.S. Simonides, C. Van Hardeveld, Biochim. Biophys. Acta 943 (1988) 349–359.
[44] L. De Meis, M.L. Bianconi, V.A. Suzano, FEBS Lett. 406 (1997) 201–204.
[45] L. De Meis, J. Physiol. 274 (1998) C1738–C1744.